

FLOWGEN: Fast and slow graph generation

Aman Madaan¹ Yiming Yang¹

Abstract

Machine learning systems typically apply the same model to both easy and tough cases. This is in stark contrast with humans, who tend to evoke either *fast* (instinctive) or *slow* (analytical) thinking process, depending on the difficulty of the problem, as a property called the dual-process theory of mind. We present FLOWGEN, a graph-generation model inspired by the dual-process theory of mind. Depending on the difficulty of graph completion at the current step, the system either call a FAST (weaker) module or a SLOW (stronger) module for the task. These modules have identical architectures, but vary in the number of parameters and consequently differ in generative power. Experiments on real-world graphs show that FLOWGEN can successfully generate graphs similar to those generated by a single large model, while being two-times faster.

1. Introduction

Graphs provide a rich abstraction for a wide range of tasks including molecular design (De Cao & Kipf, 2018; Samanta et al., 2019; Lim et al., 2020), chemical compound design (Lim et al., 2020), online user interaction modeling (Zhou et al., 2020a), and map layout design (Mi et al., 2021). Developing generative models of graphs is therefore an important classical problem, which has seen renewed interest with the success of deep learning models. Specifically, *implicit* generative models are a popular choice for graph generative modeling. Unlike explicit models, implicit generative models do not explicitly model the distribution of graphs but instead allow sampling graphs. A popular example of such implicit models are GANs, and have recently shown state of the art results for generative modeling of graphs (Bojchevski et al., 2018).

¹Language Technologies Institute, Carnegie Mellon University, Pittsburgh, PA. Correspondence to: Aman Madaan <amadaan@cs.cmu.edu>.

Like typical machine learning models, generative models of graphs currently use identical model complexity and computational strength while generating graphs. However, since these models are constructive by design (i.e., they build a graph piece-by-piece), it is natural to expect that generating different parts of a graph requires different levels of reasoning. For example, generating a 2-hop neighborhood frequently seen during training might be *easier* than generating a novel 4-hop neighborhood.

Indeed, it has long been posited (Posner & Snyder, 1975; Shiffrin & Schneider, 1977; Evans, 1984; Stanovich, 2000; Kahneman, 2003; Frankish, 2010) that humans frequently use differential reasoning based on the problem difficulty. For example, consider two problems: i) $2 * 2 = ?$, and ii) $203 * 197 = ?$. Both these problems involve multiplication between two integers. Yet, they pose a very different level of difficulty for a human solver. The answer to $2*2$ will almost instinctively come to most, while solving $19*3$ will require more careful thinking. Specifically, Stanovich (2000) propose to divide mental processing as being done by two metaphorical systems referred by them as *System 1* (instinctive, used for $2 * 2$) and *System 2* (analytical, planner, used for $203 * 197$). The terms FAST and SLOW for Systems 1 and 2 were subsequently popularized by Kahneman (2011). There is now a growing interest in utilizing a combination of fast and slow reasoning systems in diverse areas of Machine Learning (Anthony et al., 2017; Mujika et al., 2017; Schwarzschild et al., 2021b).

This paper introduces FLOWGEN, a generative graph model that is inspired by the dual-process theory of mind. FLOWGEN decomposes the problem of generating a graph into the problem of learning to generate walks. Generating walks provides a setting where identifying the easy and challenging portions is easier: starting from a given node, the model begins by generating walks seen during the training in known neighborhoods. The difficulty of generating such walks then gradually increases for two reasons. First, conditioning on increasingly longer contexts is required for generating longer walks. Second, as the length of the walks exceeds the length seen during training, a model is forced to create neighborhoods not seen during the training: a task that requires more robust generalization capabilities. FLOWGEN leverages this mismatch in problem difficulty by dynamically switching from a small (FAST) model to a

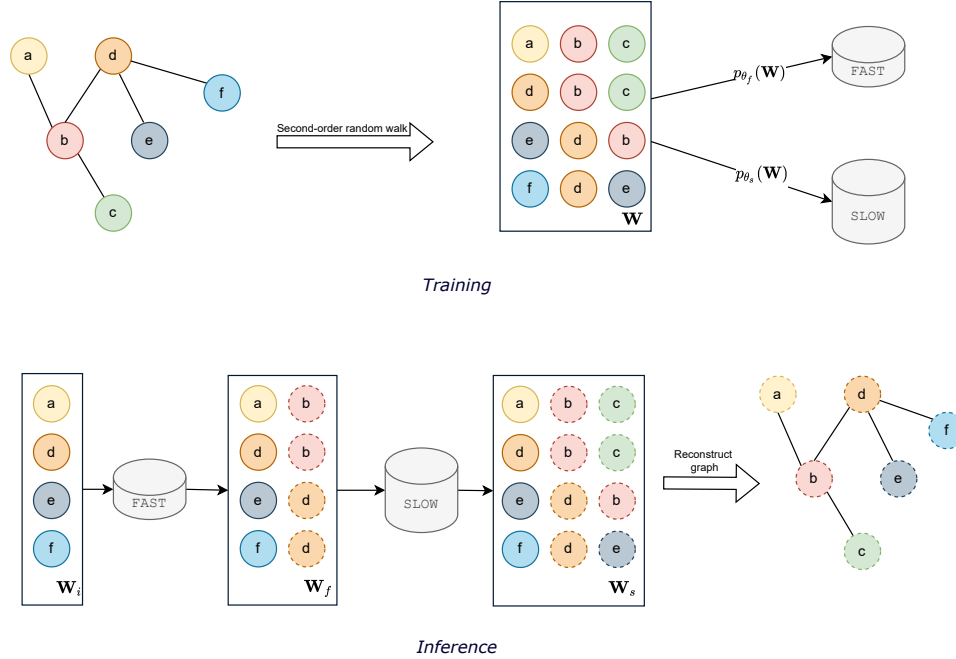


Figure 1. An overview of FLOWGEN: During training (top, Section 2.1), two auto-regressive models (FAST and SLOW) are trained on a corpus of random walks. The two models have the same architecture, but differ in size (number of parameters). During inference (below, Section 2.2), the two models are used in tandem for generating a graph. The FAST model generates the simpler, initial parts of the walk, and the SLOW model takes over for generating the latter, more challenging parts.

large (SLOW) model for efficient graph generation. Figure 1 provides an overview of our approach. FLOWGEN method achieves the same results as using the SLOW method alone on three different graphs, while taking up to 50% less time.

The backbone of FLOWGEN is a decoder-only transformer model, similar to the architectures used by the popular GPT2 models. Using transformers allows us to easily instantiate fast and slow versions of the same model by varying the number of layers. In contrast to the state-of-the-art methods for generative modeling of graphs that use either an implicit model (e.g., GANs as done by Bojchevski et al. (2018)), explicit graph distributions (with no option to vary the parameterization), or generate an entire graph sequence and leverage graph-aware decoding methods (You et al., 2018), our method is simpler (based on a standard transformer language model) and not sensitive to hyper-parameters (an identical network setup achieves gains across different graphs.).

2. FLOWGEN

In this section, we describe our novel graph generation method. First, we describe how auto-regressive models can be used for graph generation. Next, we describe how we use two of these models for dynamically for efficient graph generation.

2.1. Graph generation using auto-regressive models

Notation We denote a graph by \mathcal{G} . A random walk w is a sequence of k nodes v_1, v_2, \dots, v_k obtained by traversing the \mathcal{G} for k steps starting from v_1 . A random walk matrix of m such walks is denoted by $\mathbf{W} \in \mathbb{R}^{m \times k}$. An element $v_{ij} \in \mathbf{W}$ denotes the j^{th} node in the i^{th} random walk. For a single random walk w , v_i denotes the i^{th} node in w . The nodes connected to v_i are denoted by $\text{Adj}(v_i)$. We outline the key steps in training and inference (graph generation) below.

2.1.1. TRAINING

Step 1: Generating random walks for training Given a graph \mathcal{G} , we create a second-order random walk matrix $\mathbf{W} \in \mathbb{R}^{m \times k}$. The matrix \mathbf{W} contains m second-order walks, each of length k . A second-order random walk (Grover & Leskovec, 2016) helps in capturing rich topological information of the graph. Specifically, a node v_i is sampled as a function of the previous two nodes: v_{i-1} and v_{i-2} (and not just v_{i-1} , which will be the case with vanilla sampling). The details of the sampling procedure are included in Appendix B. Each walk is started by sampling a random node from \mathcal{G} .

Step 2: Training an auto-regressive model We use an auto-regressive language model p_θ to learn a generative model of the random walk matrix $p(\mathbf{W})$. Specifically, we treat \mathbf{W} as a corpus of m random walks $[w_1, w_2, \dots, w_k]$ from \mathcal{G} . The model is trained to generate the i^{th} node in the walk, conditioned on the preceding ($< i$) nodes. We model the probability $p(W)$ of a random walk as a series of conditional next token distributions: $p(\mathbf{W}) = \prod_{i=1}^m \prod_{j=1}^k p_\theta(v_{ij} \mid v_{i,<j})$. We parameterize p_θ using a decoder-only language model based on the architecture used by GPT-2 (Radford et al., 2019). The number of self-attention layers (or *depth*) of the language model decides the number of parameters θ , and, consequently, the strength of the model.

2.1.2. INFERENCE: GRAPH GENERATION

Step 3: generating random walks As the first step of inference, an approximate random walk matrix \mathbf{W}' is obtained by randomly sampling from $p(\mathbf{W})$. To sample a random walk of length l , we first generate a random node $v_1 \in \mathcal{G}$. The generation process begins by $v_2 \sim p_\theta(v \mid v_1)$. The next token is then drawn by sampling $v_3 \sim p_\theta(v \mid v_1, v_2)$. The process is repeated for $l-1$ steps to generate a random walk of size l . We generate n , and stack them to create a generated random walks matrix \mathbf{W}' .

Step 4: Reconstructing graph: We need to assemble the generated graph \mathcal{G}' from generated random walks \mathbf{W}' generated in the previous step. We follow the two-step procedure used by Bojchevski et al. (2018) to assemble the generated graph \mathcal{G}' from generated random walks \mathbf{W}' . First, \mathbf{W}' is converting to a count matrix \mathbf{S} , where S_{ij} is the number of times the nodes v_i and v_j appeared consecutively (indicating an edge between v_i and v_j). Next, an edge is added between v_i and v_j in the generated graph \mathcal{G}' with probability $p_{ij} = \frac{S_{ij}}{\sum_{v \in \text{Adj}(i)} S_{iv}}$

A note on evaluation Note that a large model may simply remember a small graph. However, our goal is not such memorization, but rather generalization. To evaluate this, $\sim 20\%$ of the edges from \mathcal{G} are hidden during training. \mathcal{G}' is then evaluated for presence of these edges.

Relation to language modeling Our graph generation method has a 1:1 correspondence with language modeling using graphs. Our method deals with a graph as characterizing a language, where each random walk \mathbf{W} in \mathcal{G} is a sentence, and each node v is a word (or token). The language model correspondingly learns to generate valid random walks from \mathcal{G} . Similar ideas were explored by Deepwalk ((Perozzi et al., 2014)) for learning informative node representations.

2.2. Fast and slow graph generation

As discussed in the previous section, our method relies on generating random walks. Let w be a random walk of length l to be generated using a trained graph generation model p_θ , starting from a random node v_1 . Since p_θ is auto-regressive, the generation process can be succinctly represented using the chain rule. Let v_k be a node in w with $1 < k < l$.

$$p_\theta(w) = \prod_{i=1}^k p_\theta(v_i \mid v_{<i}) \prod_{j=k+1}^l p_\theta(v_j \mid v_{<j}; v_1, \dots, v_k) \quad (1)$$

We posit that there is a k such that the generation of walks v_1, \dots, v_k and v_{k+1}, \dots, v_l require different levels of difficulty. Thus, it should be possible to generate the *easy* first part of the walk (v_1, \dots, v_k) using a FAST model, leaving the rest to a SLOW model.

Intuitively, it is easier to generate the first few nodes of a random walk: the first node of the walk is given (the starting point), and generating the second node requires an understanding of a second-order random walk. Generating subsequent random walks require models to pay attention to the walk seen so far and gets progressively more difficult as the walk length increases. Further, generating walks longer than k (random walk length used for training) requires a model with better generalization capabilities.

Instantiating FAST and SLOW models Our We train two different generation models (i.e., two different p_θ) using procedure outlined in Section 2.1: FAST and SLOW. Both these models have the same architecture type (transformers), but differ in the number of parameters: FAST is a 1-4 layered transformer whereas SLOW has 6 or more layers (depending on the graph). A speed vs. performance trade-off is expected for the FAST and SLOW models: FAST will struggle with generating new walks, whereas SLOW will generate these at the cost of slower inference.

Our method, FLOWGEN, relies on these key intuitions to pair a fast and slow process together. We start by generating walks using a FAST model and then switch to a SLOW model to explore novel neighborhoods. Since generation is auto-regressive, such a formulation is natural: subsequent walks can be conditioned on the walks seen so far without any changes to the two models.

2.3. Switching from FAST to SLOW

FLOWGEN proposes to generate the *first* part of the walk quickly using FAST, and the remaining part slowly but more accurately using SLOW. A critical decision for FLOWGEN is the *handover* point: at what point should the generation switch from using FAST to SLOW? While generating a walk

of length l , the switch from FAST to SLOW can happen at any point v_j , where $j \in (0, l)$. However, the choice of v_j is important due to the speed vs. accuracy trade-off: a large j implies that the walk will be generated quickly but mainly using the FAST model. On the other hand, a smaller j will shift most of the responsibility to the SLOW model, for better accuracy but slower inference. To characterize the difference in performance, we need the notion of a neighborhood, and random walks that perform exploration and exploitation.

- **Neighborhood \mathcal{N} :** a consecutive sequence of p nodes that appear in a random walk. For instance, given a random walk $(v_1, v_2, v_3, v_4, v_5)$, and $p = 4$, the two neighborhoods are (v_1, v_2, v_3, v_4) and (v_2, v_3, v_4, v_5) .
- **Exploration and exploitation:** a random walk w to be in a state of *exploration* if it is in a neighborhood where it is discovering new neighborhoods not present in the training data. Otherwise, the walk is said to be in the *exploitation* phase. As mentioned earlier, a random walk starts from a given node, and thus is expected to be in exploitation mode in the beginning (known neighborhoods), before switching to exploration mode (new neighborhoods). Both exploration and exploitation phases are essential: exploration helps the model generalize to new edges, whereas exploitation helps the model recreate the structure.

Given these definitions, a sweet spot for the handover point v_j will be the step where the random walk exits the exploration mode and enters the exploitation mode. To perform this check efficiently, we create a *bloom filter* (Bloom, 1970) of all the neighborhoods seen in the training data.

Detecting exploration vs. exploitation Given a random walk w , an initial attempt to detect exploration vs. exploitation would be to check if each neighborhood in w is in the training data. In principle, this can be done by first creating a set of all possible neighborhoods \mathbb{N} of size p in the training data (m random walks of length k): $\mathbb{N} = \{(v_{ij}, v_{i,j+1}, \dots, v_{i,j+p}) \mid i \in [1, m], j \in [1, k - p + 1]\}$. Next, a balanced binary tree (available in most programming languages as a hashmap) populated with \mathbb{N} can be used to efficiently answer membership queries over \mathbb{N} , allowing us to detect exploration vs. exploitation. In practice, this approach is intractable as the number of all possible p neighborhoods may be exponential.

Using solutions like distributed caching is possible, but may add additional overhead that can cancel any gains obtained using a mix of FAST and SLOW models. Instead, we note that our setup requires a data structure that is less powerful than a hashmap, and allows us to make two concessions: i) we are only interested in checking if a particular neighborhood is absent in the graph, and thus require a reduced set

of functions as compared to those supported by a hashmap, and ii) the decision is used to switch to a better (SLOW) model, and thus some degree of error is tolerable. Fortunately, bloom filters exist (Bloom, 1970) are widely used for precisely these use cases.

Bloom filter A bloom filter \mathcal{B} created over a set \mathbb{S} provides an efficient way to check if a key x does not exist in \mathbb{S} . Bloom filters are particularly useful in data-intensive applications, where an application might want to be sure about a query’s existence before checking an off-line database (Broder & Mitzenmacher, 2004; Kleppmann, 2017).

Given a search key x , if the search over \mathcal{B} is unsuccessful, it is guaranteed that $x \notin \mathbb{S}$. Otherwise, x may be present with a probability $1 - P$, where P is the false positive rate. Internally, a bloom filter \mathcal{B} is implemented as an array of M bits accompanied by h hash functions H_1, H_2, \dots, H_h . To add an element $x \in \mathbb{S}$ to \mathcal{B} , each of the h hash functions map x to $[1, M]$, and thus the corresponding bits are set to 1. Concretely, $\mathcal{B}[H_i(x)] = 1 \forall i \in [1, h]$.

To check the presence of an element x in \mathcal{B} , it suffices to check if $\exists i \in [1, h] \mathcal{B}[H_i(x)] = 0$. If so, then it is guaranteed that $x \notin \mathbb{S}$ (otherwise, all the bits would be set to 1). Otherwise, the element *may be* present. Crucially, while creating the bloom filter incurs a one-time cost of $\mathcal{O}(|\mathbb{S}|h)$, the lookup can be done in $\mathcal{O}(h)$ time. Combined with the space requirements for \mathcal{B} , $M \ll |\mathbb{S}|$, a bloom filter provides an efficient way to determine if an element is absent from a set.

We use an implementation of scalable bloom filters (Almeida et al., 2007), which are more robust to false positives than the vanilla implementation. For this implementation, it can be shown that $c \approx M \frac{\log 2^2}{|\log P|}$, where c is the capacity, or the maximum number of elements in \mathbb{S} that a \mathcal{B} with M can support while keeping the false positive rate $\leq P$. For completeness, we have included a detailed analysis and relevant algorithms in Appendix A.

Bloom filter of neighborhoods As noted in Section 2.1, we generate 100M (second-order) random walks of length 16 for each graph. We re-use these walks to create a bloom filter \mathcal{B} . For each walk, we use a sliding window of length $p = 4$ and inserted the neighborhood in \mathcal{B} . Note that this is a one-time procedure. Using a false-positive rate of $P = 0.01$, the \mathcal{B} is approximately $130\times$ smaller than saving the neighborhoods in a hashmap on average. Notably, the creation procedure is one-time, and lookup time is a small constant.

Given \mathcal{B} , we still need to determine the switching point. Thus, we sample $50k$ walks using both the FAST and SLOW models. During generation, we query \mathcal{B} with the current neighborhood (the most recent p nodes), and mark the cur-

rent phase as exploration or exploitation accordingly.

Figure 2 shows for each timestep, and the % of times the random walk was in exploration mode for both FAST and SLOW models. At the beginning of the walk, the model tends to stick to the same neighborhood (low exploration %). The degree of exploration slowly increases as the walk reaches k . Then, the model explores new neighborhoods for both FAST and SLOW models. Crucially, note that the extent of exploration is much more significant for the SLOW model. We set the j point to be the timestep where the rate of change of exploration is the greatest: $j = \arg \max_i \frac{dEX(i)}{dt}$. The point is detected using <https://pypi.org/project/kneed/>.

In summary, FLOWGEN combines *learning* (by training FAST and SLOW models) with search (by using \mathcal{B} to locate optimal handover point) to generate a system that can adapt to the difficulty of the problem for efficient graph generation.

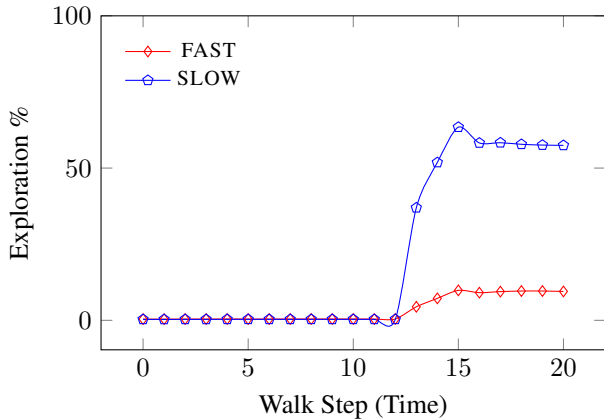


Figure 2. Exploration % (y-axis) vs. random walk step for CORAML. The larger SLOW model explores once the walk exceeds a certain threshold, whereas the lighter FAST model repeats the training data.

Calculating handover point We calculate the handover point (the step where we switch from FAST to SLOW) for each graph separately. We create a bloom filter \mathcal{B} using all the four-node neighborhoods in the training data. For each graph, we generate 10,000 random walks of length $l = 24$ using both FAST and SLOW models. Then, the handover point is calculated by finding the *knee* of the exploration % curve, and we use Satopaa et al. (2011) to find such points.¹. We plot the % of neighborhoods not found in \mathcal{B} (or exploration %) in Figure 2 for CORAML.

For all the graphs, the FAST model does little exploration. Notably, the effect is more pronounced for larger graph POLBLOGS, which proves to be especially challenging for

the FAST model (Figure 5 in Appendix).

We also experiment with using entropy for deciding the switch, but found it ineffective in determining exploration vs. exploitation Appendix (C.3), in line with prior work that shows that language models are typically not well-calibrated (Jiang et al., 2021).

3. Experiments

In this section, we establish the efficacy of our approach with experiments. First, we show that autoregressive models of graphs can be learned successfully with language models. Next, we present the results from experiments with FAST and SLOW modeling.

Graphs We experiment with four representative large graphs: graphs formed by citation networks (CITSEER (Sen et al., 2008), CORAML (Mccallum, 2008)), political blogs (POLBLOGS (Adamic & Glance, 2005)), and citation-network for medical publications related to diabetes (PUBMED (Sen et al., 2008))) on which implicit graph generation models are shown to perform well.

Graph statistics are provided in Table 1. For the link prediction experiments, we use the train/test/val splits provided by Bojchevski et al. (2018).

	CORAML	CITSEER	POLBLOGS	PUBMED
N_{LCC}	2,810	2,110	1,222	19,717
E_{LCC}	7,981	3,757	16,714	51,913

Table 1. Graphs statistics. The N_{LCC} and E_{LCC} refer to the number of nodes and edges in the largest connected component. We use the dataset supplied by Bojchevski et al. (2018) for all experiments. The results for

Tasks and metrics Our goal is to learn a generative model of large graphs. Following prior work, we focus on two different evaluation measures, focused on measuring the ability of the model to learn graph structure and the ability to generalize.

- **Generalization:** a large model may simply *remember* all the random walks seen during training. Thus, the structural metrics are not sufficient for distinguishing between a model that has learned to generalize and a model that is overfitting to the input graph. We follow prior work and evaluate generalization via a link prediction task as a remedy. During training, about 20% of the edges from each graph are not included in the training data. The reconstructed graph \mathcal{G}' is evaluated to check if these edges are contained. Intuitively, a model that generalizes over the graph instead of regurgitating the training data will perform better when generating un-

¹<https://pypi.org/project/kneed/>

seen edges. Link prediction is evaluated using average precision and AUC score, where we use implementation provided by scikit-learn (Pedregosa et al., 2011) for calculating AUC score.² Recall that the graph is reconstructed from the generated random walks (Section 2.1). p_{ij} , the normalized probability of an edge between nodes i and j , is estimated from the count matrix and supplied to the `roc_auc_score` function as y_{pred} .

- **Structure:** to evaluate graph structure, we additionally calculate the topological properties of the graph, including the maximum degree, associativity, triangle count, and power-law exp. A detailed definition of these metrics is provided in Section C.1 for completeness.

FAST, SLOW, and FLOWGEN models We base FLOWGEN on a decoder-only transformer architecture. Specifically, we use a layered-transformer architecture with stacks of self-attention layers (SA). Each SA layer comprises a self-attention (Vaswani et al., 2017), along with a feed-forward layer and skip connections. To recall from Section 2.2, our experiments involve three models: 1.) SLOW: larger model with six layers for all datasets except PUBMED, where it has 36 layers. 2.) FAST: smaller model with a single layer for all datasets, and has 6 layers for PUBMED, and 3.) FLOWGEN: a combination of FAST and SLOW. FAST and SLOW models are separately trained, and are combined during inference: the first part of the random walk generation is done with FAST, and the second half with SLOW.

Other than using larger FAST and SLOW models for PUBMED, we do not perform any hyper-parameter tuning: all the models use the same hyperparameters. We consider the lack of hyper-parameter tuning a core strength of our approach and a key advantage with respect to the baseline. We do not perform any hyper-parameter tuning: all the models use the same hyperparameters, and use a single Nvidia 2080-ti for all experiments.

Baselines Note that the main goal of this work is to show that FAST and SLOW models can be combined for effective graph generation. Nonetheless find that FLOWGEN is competitive with existing graph-generation methods (Section 3.1), notably NetGAN (Bojchevski et al., 2018). For completeness, we also compare with a number of parametric, non-parametric, and graph-specific baselines including degree-corrected stochastic block model (DC-SBM (Karrer & Newman, 2011)), degree-centrality based adamic-adar index (AA index (Adamic & Adar, 2003)), variational graph autoencoder (Kipf & Welling, 2016), and Node2Vec (Grover

²We used implementation at: https://scikit-learn.org/stable/modules/generated/sklearn.metrics.roc_auc_score.html#sklearn.metrics.roc_auc_score

Graph	Max. degree	Assortativity	Triangle Count	Power law exp.	Intra-community density
CORA-ML	240	-0.075	2,814	1.860	4.3e-4
Netgan	233	-0.066	1,588	1.793	6.0e-4
FAST	216	-0.082	2,461	1.84	5.8e-4
SLOW	200	-0.079	2,143	1.853	5.4e-4
FLOWGEN	200	-0.080	2,351	1.84	5.6e-4

Table 2. Comparison of SLOW, FAST, and FLOWGEN with Netgan (Bojchevski et al., 2018) for structural metrics for CORAML. The ground truth values are listed in the top-row, and the value closer to the ground truth is highlighted in bold. All variants closely match the ground truth graph across a range of metrics.

Method	CORAML	CITSEER	PUBMED	POLBLOGS
AA-index	92.16	88.69	84.98	85.43
DC-SBM	96.03	94.77	96.76	95.46
Node2Vec	92.19	95.29	96.49	85.10
VGAE	95.79	95.11	94.50	93.73
NetGAN	95.19	96.30	93.41	95.51
FLOWGEN	96.90	96.50	93.00	93.80

Table 3. Comparison of our SLOW model with other graph generation baselines on link prediction task. Our graph generation model is competitive. Results for SLOW and FAST models are listed in Table 4. We find identical trends with average precision and other metrics, results in Section C, Table 7.

& Leskovec, 2016).

3.1. RQ1: Can auto-regressive language models successfully learn generative models of graphs?

In contrast with prior work, our backbone graph-generation model is a simple transformer-based language model. The simplicity of this method allows us to experiment with the fast and slow settings easily. However, does this simplicity come at the cost of performance? To establish that our graph-generation model is competitive, we evaluate the performance of the larger model, SLOW, for link prediction and structural generation for all the graphs.

The results in Table 2 and 3 show that our transformer-based random walk models achieves competitive performance compared with methods based on either adversarial training or latent variable approaches. We include additional results on structural prediction in Section C. Next, we experiment with FLOWGEN, which combines FAST and SLOW graphs for generation.

3.2. RQ2: is FLOWGEN effective for graph-generation?

Instead of using a fixed handover point, we can also switch dynamically at each step. However, we found that constantly switching between models incurs a cost as the model has to

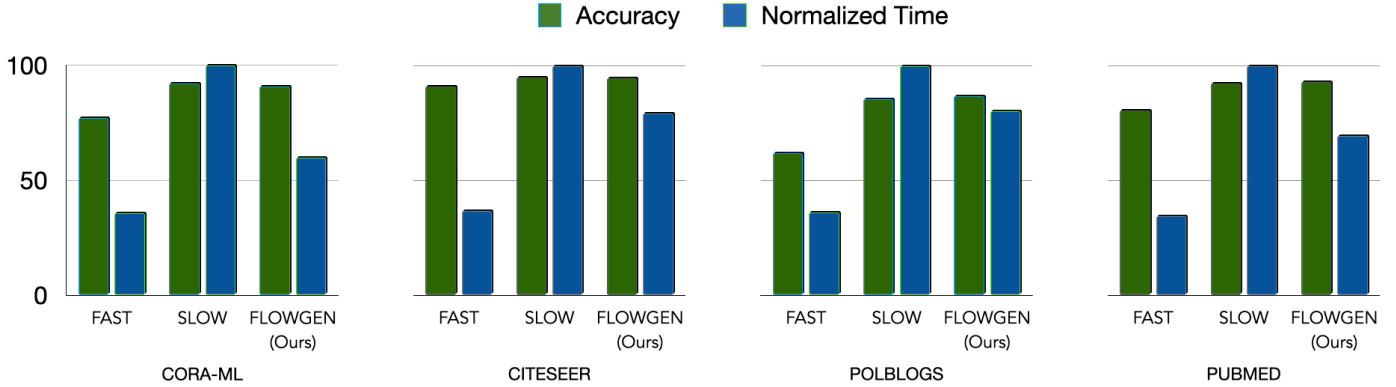


Figure 3. **Main results:** AUC and time for the different graphs using FAST, SLOW, and FLOWGEN: FLOWGEN is competitive with the larger SLOW model, while being upto 2x faster.

	FAST		SLOW		FLOWGEN	
	AUC	Time	AUC	Time	AUC	Time
CORAML	91.5	50k	96.7	180k	96.9	110k
CITESEER	96.1	62k	96.8	172k	96.5	137k
PUBMED	80.5	253k	92.1	735k	93.0	509k
POLBLOGS	66.2	48k	93.8	156k	93.8	108k

Table 4. AUC (\uparrow) for FAST, SLOW, and FLOWGEN. The Time (seconds, \downarrow) taken by each setup is in parentheses. FLOWGEN closely matches or outperforms the larger model SLOW while taking a fraction of time.

perform a forward pass on all the tokens seen so far. This is required, as the auto-regressive attention at each step depends on the hidden layer representations for all layers and previous steps. A static handover point avoids constant switching and does not degrade the performance.

Results The results are shown in Table 4 and Figure 3. While SLOW model outperforms FLOWGEN marginally on CORAML and CITESEER, the trade-off is clear from Table 4: FLOWGEN take considerably less time to achieve similar or better accuracy. The size of the underlying graph also plays a role in how significant the gains are from our approach: FLOWGEN outperforms the SLOW model for the large POLBLOGS graphs. In contrast, the FAST model is competitive for a smaller graph like CITESEER. We include additional results in Section C.

Selection of handover point We use a fixed switching point of 13 for all the graphs. Is this a key design choice? Will delaying the switching point lead to more accurate graphs that are generated slowly? While overall results show that is indeed the case, we conduct a fine-grained analysis of switching point choice for CORAML. The results

are shown in Figure 4. We find that selection of handover point is indeed important.

Performance of FLOWGEN with scale How does the performance of FLOWGEN change as the scale of data increases? We show in Section C.2 that FLOWGEN matches or outperforms SLOW consistently as the number of walks is increased from 500k to 100m (used current experiments).

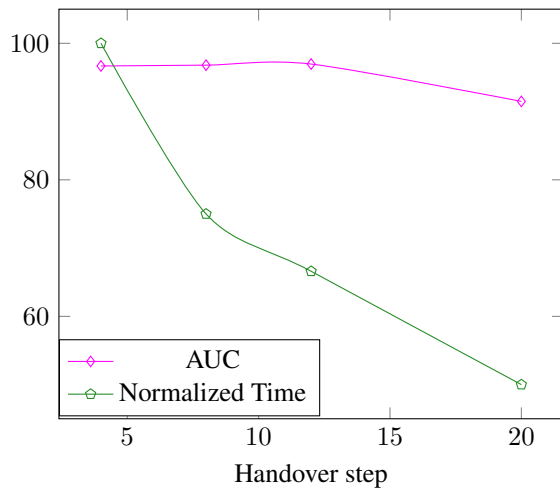


Figure 4. AUC and Normalized time for different choices of handover step. When handover to SLOW model happens early in the walk (step 4), the time taken is ~ 720 seconds for generating 500 walks, at AUC of $\sim 97\%$. Delaying the switch to step 20 leads to a 2x reduction in time taken to generate the walk (360 seconds), with a considerably reduced AUC of 91%. FLOWGEN offers a tradeoff by calculating the optimal switching point.

4. Related Work

Graph generation Our work relies on using random walks for learning generative models of graph, similar to (Bojchevski et al., 2018) and (You et al., 2018). (You et al., 2018) learn a generative model of molecules, where each inference step generates the complete graph. Their setup also leverages graph-aware specialized decoding procedures, and scales for their setup since molecular graphs are typically small. In contrast, our random walk based method allows learning generative models of large graphs that cannot be generated in a single inference step. Additionally, in contrast with (Bojchevski et al., 2018) that use GAN-based training, we leverage relatively simple graph generation model. The idea of modeling random walks as sequence of nodes is identical to DeepWalk (Perozzi et al., 2014). However, different from DeepWalk, our main goal is generative graph modeling, and not learning node representations. Further, our underlying architecture (transformers) is also different than the one used by DeepWalk (MLP).

Fast and slow machine learning There are several works that use the fast-slow metaphor. For instance, Mujika et al. (2017) present a hierarchical RNN architecture, where the lower (or fast) layer contains one RNN cell for each time-step. The higher layer in contrast connects several different neurons together. Hill et al. (2020) focus on language reasoning tasks, where slow and fast denote the two phases of learning: slow supervised training, and a fast k-shot adaptation.

Our work is closest in spirit to the remarkable recent work by Schwarzschild et al. (2021b;a), who focus on three different generalization tasks. They observe increasing the number of test iterations (which corresponds to the network depth in their setting) helps the models in generalizing better to the difficult problem. Our study replicates this general finding, by showing that FAST (small) and SLOW (larger) models can be combined for efficient graph generation. Our method can be seen as an extension of their method for graph generation, with the following novel additions. First, instead of varying the depth of the network, we actually leverage two different transformer networks (FAST and SLOW), and the output of FAST is used by SLOW. Second, we determine the switching point in a principled fashion using bloom filters. Schwarzschild et al. (2021b) note that the confidence of the model was a good proxy for correctness in their setting. We find that not to be the case, and also propose a method for finding a switching point for the network.

Adaptive computation A related body of work on adaptive computation seeks to preempt computation based on intermediate representations (Liu et al., 2020; Zhou et al., 2020b; Schuster et al., 2021; Geng et al., 2021). Different from these methods, our approach completely obviates mak-

ing any architectural modifications. As the attached code shows, the FAST and SLOW models are initialized identically, with the difference of the number of layers. The switch from FAST to SLOW is also simple: FLOWGEN moves intermediate outputs from a FAST to a SLOW model at an optimal step, and the auto-regressive nature of our graph generation setup guarantees that the setup remains well-defined. Schuster et al. (2022) present CLAM, a language model that performs language generation adaptively. In

5. Conclusion

Future machine learning applications will potentially have API-level access to several models of varying strengths and costs of usage. In such scenarios, building systems that can adapt to the difficulty of the sample will be critical for scale and efficiency. FLOWGEN presents a real-world use case for such FAST-SLOW systems. As future work, we plan to explore the use of FAST-SLOW generation methods for effective and adaptive language generation using large-language models.

Acknowledgment

This material is partly based on research sponsored in part by the Air Force Research Laboratory under agreement number FA8750-19-2-0200. The U.S. Government is authorized to reproduce and distribute reprints for Governmental purposes notwithstanding any copyright notation thereon. The views and conclusions contained herein are those of the authors and should not be interpreted as necessarily representing the official policies or endorsements, either expressed or implied, of the Air Force Research Laboratory or the U.S. Government.

References

- Adamic, L. A. and Adar, E. Friends and neighbors on the web. *Social networks*, 25(3):211–230, 2003.
- Adamic, L. A. and Glance, N. The political blogosphere and the 2004 us election: divided they blog. In *Proceedings of the 3rd international workshop on Link discovery*, pp. 36–43, 2005.
- Almeida, P. S., Baquero, C., Preguiça, N., and Hutchison, D. Scalable bloom filters. *Information Processing Letters*, 101(6):255–261, 2007.
- Anthony, T., Tian, Z., and Barber, D. Thinking Fast and Slow with Deep Learning and Tree Search. In *Advances in Neural Information Processing Systems*, volume 30. Curran Associates, Inc., 2017. URL <https://proceedings.neurips.cc/paper/2017/hash/d8e1344e27a5b08cdfd5d027d9b8d6de-Abstract.html>.
- Bloom, B. H. Space/time trade-offs in hash coding with allowable errors. *Communications of the ACM*, 13(7):422–426, 1970.
- Bojchevski, A., Shchur, O., Zügner, D., and Günnemann, S. Netgan: Generating graphs via random walks. In *International Conference on Machine Learning*, pp. 610–619. PMLR, 2018.
- Broder, A. and Mitzenmacher, M. Network applications of bloom filters: A survey. *Internet mathematics*, 1(4):485–509, 2004.
- Chang, F., Feng, W.-c., and Li, K. Approximate caches for packet classification. In *IEEE INFOCOM 2004*, volume 4, pp. 2196–2207. IEEE, 2004.
- Christensen, K., Roginsky, A., and Jimeno, M. A new analysis of the false positive rate of a bloom filter. *Information Processing Letters*, 110(21):944–949, 2010.
- De Cao, N. and Kipf, T. MolGAN: An implicit generative model for small molecular graphs. *arXiv:1805.11973 [cs, stat]*, May 2018. URL <http://arxiv.org/abs/1805.11973>. arXiv: 1805.11973.
- Evans, J. S. B. T. Heuristic and analytic processes in reasoning*. *British Journal of Psychology*, 75(4):451–468, 1984. ISSN 2044-8295. doi: 10.1111/j.2044-8295.1984.tb01915.x. URL <https://onlinelibrary.wiley.com/doi/abs/10.1111/j.2044-8295.1984.tb01915.x>. eprint: <https://onlinelibrary.wiley.com/doi/pdf/10.1111/j.2044-8295.1984.tb01915.x>.
- Frankish, K. Dual-Process and Dual-System Theories of Reasoning. *Philosophy Compass*, 5(10):914–926, 2010. ISSN 1747-9991. doi: 10.1111/j.1747-9991.2010.00330.x. URL <https://onlinelibrary.wiley.com/doi/abs/10.1111/j.1747-9991.2010.00330.x>. eprint: <https://onlinelibrary.wiley.com/doi/pdf/10.1111/j.1747-9991.2010.00330.x>.
- Geng, S., Gao, P., Fu, Z., and Zhang, Y. Romebert: Robust training of multi-exit bert. *arXiv preprint arXiv:2101.09755*, 2021.
- Grover, A. and Leskovec, J. node2vec: Scalable Feature Learning for Networks. *arXiv:1607.00653 [cs, stat]*, July 2016. URL <http://arxiv.org/abs/1607.00653>. arXiv: 1607.00653.
- Hill, F., Tieleman, O., von Glehn, T., Wong, N., Merzic, H., and Clark, S. Grounded Language Learning Fast and Slow. *arXiv:2009.01719 [cs]*, October 2020. URL <http://arxiv.org/abs/2009.01719>. arXiv: 2009.01719.
- Jiang, Z., Araki, J., Ding, H., and Neubig, G. How Can We Know When Language Models Know? On the Calibration of Language Models for Question Answering. *Transactions of the Association for Computational Linguistics*, 9:962–977, September 2021. ISSN 2307-387X. doi: 10.1162/tacl_a_00407. URL https://doi.org/10.1162/tacl_a_00407.
- Kahneman, D. Maps of Bounded Rationality: Psychology for Behavioral Economics. *The American Economic Review*, 93(5):1449–1475, 2003. ISSN 0002-8282. URL <https://www.jstor.org/stable/3132137>. Publisher: American Economic Association.
- Kahneman, D. *Thinking, fast and slow*. Macmillan, 2011.
- Karrer, B. and Newman, M. E. Stochastic blockmodels and community structure in networks. *Physical review E*, 83(1):016107, 2011.
- Kipf, T. N. and Welling, M. Variational graph auto-encoders. *arXiv preprint arXiv:1611.07308*, 2016.
- Kleppmann, M. *Designing data-intensive applications: The big ideas behind reliable, scalable, and maintainable systems*. ” O’Reilly Media, Inc.”, 2017.
- Lim, J., Hwang, S.-Y., Moon, S., Kim, S., and Youn Kim, W. Scaffold-based molecular design with a graph generative model. *Chemical Science*, 11(4):1153–1164, 2020. doi: 10.1039/C9SC04503A. URL <https://pubs.rsc.org/en/content/articlelanding/2020/sc/c9sc04503a>. Publisher: Royal Society of Chemistry.

- Liu, W., Zhou, P., Wang, Z., Zhao, Z., Deng, H., and Ju, Q. Fastbert: a self-distilling bert with adaptive inference time. In Proceedings of the 58th Annual Meeting of the Association for Computational Linguistics, pp. 6035–6044, 2020.
- Mccallum, A. K. Automating the Construction of Internet Portals with Machine Learning. pp. 37, 2008.
- Mi, L., Zhao, H., Nash, C., Jin, X., Gao, J., Sun, C., Schmid, C., Shavit, N., Chai, Y., and Anguelov, D. HDMapGen: A Hierarchical Graph Generative Model of High Definition Maps. In 2021 IEEE/CVF Conference on Computer Vision and Pattern Recognition (CVPR), pp. 4225–4234, Nashville, TN, USA, June 2021. IEEE. ISBN 978-1-66544-509-2. doi: 10.1109/CVPR46437.2021.00421. URL <https://ieeexplore.ieee.org/document/9577586/>.
- Mujika, A., Meier, F., and Steger, A. Fast-Slow Recurrent Neural Networks. In Advances in Neural Information Processing Systems, volume 30. Curran Associates, Inc., 2017. URL <https://proceedings.neurips.cc/paper/2017/hash/e4a93f0332b2519177ed55741ea4e5e7-Abstract.html>.
- Pedregosa, F., Varoquaux, G., Gramfort, A., Michel, V., Thirion, B., Grisel, O., Blondel, M., Prettenhofer, P., Weiss, R., Dubourg, V., Vanderplas, J., Passos, A., Cournapeau, D., Brucher, M., Perrot, M., and Duchesnay, E. Scikit-learn: Machine learning in Python. Journal of Machine Learning Research, 12:2825–2830, 2011.
- Perozzi, B., Al-Rfou, R., and Skiena, S. Deepwalk: On-line learning of social representations. In Proceedings of the 20th ACM SIGKDD international conference on Knowledge discovery and data mining, pp. 701–710, 2014.
- Posner, M. I. and Snyder, C. R. Attention and cognitive control. 1975.
- Radford, A., Wu, J., Child, R., Luan, D., Amodei, D., Sutskever, I., et al. Language models are unsupervised multitask learners. OpenAI blog, 1(8):9, 2019.
- Samanta, B., De, A., Jana, G., Chattaraj, P. K., Ganguly, N., and Rodriguez, M. G. NeVAE: A Deep Generative Model for Molecular Graphs. Proceedings of the AAAI Conference on Artificial Intelligence, 33:1110–1117, July 2019. ISSN 2374-3468, 2159-5399. doi: 10.1609/aaai.v33i01.33011110. URL <https://aaai.org/ojs/index.php/AAAI/article/view/3903>.
- Satopaa, V., Albrecht, J., Irwin, D., and Raghavan, B. Finding a” kneedle” in a haystack: Detecting knee points in system behavior. In 2011 31st international conference on distributed computing systems workshops, pp. 166–171. IEEE, 2011.
- Schuster, T., Fisch, A., Jaakkola, T., and Barzilay, R. Consistent accelerated inference via confident adaptive transformers. In Proceedings of the 2021 Conference on Empirical Methods in Natural Language Processing, pp. 4962–4979, 2021.
- Schuster, T., Fisch, A., Gupta, J., Dehghani, M., Bahri, D., Tran, V. Q., Tay, Y., and Metzler, D. Confident adaptive language modeling. arXiv preprint arXiv:2207.07061, 2022.
- Schwarzschild, A., Borgnia, E., Gupta, A., Bansal, A., Emam, Z., Huang, F., Goldblum, M., and Goldstein, T. Datasets for Studying Generalization from Easy to Hard Examples. arXiv:2108.06011 [cs], September 2021a. URL <http://arxiv.org/abs/2108.06011>. arXiv: 2108.06011.
- Schwarzschild, A., Borgnia, E., Gupta, A., Huang, F., Vishkin, U., Goldblum, M., and Goldstein, T. Can You Learn an Algorithm? Generalizing from Easy to Hard Problems with Recurrent Networks. In Advances in Neural Information Processing Systems, volume 34, pp. 6695–6706. Curran Associates, Inc., 2021b. URL <https://proceedings.neurips.cc/paper/2021/hash/3501672ebc68a5524629080e3ef60aef-Abstract.html>.
- Sen, P., Namata, G., Bilgic, M., Getoor, L., Galligher, B., and Eliassi-Rad, T. Collective classification in network data. AI magazine, 29(3):93–93, 2008.
- Shiffrin, R. M. and Schneider, W. Controlled and automatic human information processing: Ii. perceptual learning, automatic attending and a general theory. Psychological Review, 84:127–190, 1977.
- Stanovich, K. E. Individual differences in reasoning: Implications for the rationality debate? BEHAVIORAL AND BRAIN SCIENCES, pp. 82, 2000.
- Vaswani, A., Shazeer, N., Parmar, N., Uszkoreit, J., Jones, L., Gomez, A. N., Kaiser, L., and Polosukhin, I. Attention is all you need. In NIPS, 2017.
- You, J., Ying, R., Ren, X., Hamilton, W., and Leskovec, J. Graphrnn: Generating realistic graphs with deep auto-regressive models. In International Conference on Machine Learning, pp. 5708–5717. PMLR, 2018.
- Zhou, D., Zheng, L., Han, J., and He, J. A Data-Driven Graph Generative Model for Temporal Interaction Networks. In Proceedings of the 26th ACM SIGKDD International Conference on Knowledge Discovery &

Data Mining, pp. 401–411, Virtual Event CA USA, August 2020a. ACM. ISBN 978-1-4503-7998-4. doi: 10.1145/3394486.3403082. URL <https://dl.acm.org/doi/10.1145/3394486.3403082>.

Zhou, W., Xu, C., Ge, T., McAuley, J., Xu, K., and Wei, F. Bert loses patience: Fast and robust inference with early exit. Advances in Neural Information Processing Systems, 33:18330–18341, 2020b.

A. Overview of Bloom Filters

Algorithm 1 Creating a bloom filter with M bits and h hash functions \mathbf{H} over a set \mathbb{S} . Each hash function takes $\mathcal{O}(1)$, and thus creating a bloom filter incurs a one time cost $\mathcal{O}(h|\mathbb{S}|)$.

Given: $\mathcal{B}, \mathbf{H}, \mathbb{S}$
Init: $\mathcal{B}(i) \leftarrow 0; i \in [1, M]$
for $q \in \mathbb{S}$ **do** // $\mathcal{O}(|\mathbb{S}|)$
 for $i \leftarrow 1, 2, \dots, h$ **do** // $\mathcal{O}(|\mathbf{H}|) = \mathcal{O}(h)$
 $\mathcal{B}(\mathbf{H}_i(q)) \leftarrow 1$
 end
end

A bloom filter \mathcal{B} over a set \mathbb{S} is a data structure for efficient set-membership queries. The time to search is independent of the number of elements in \mathbb{S} . As a trade-off, a bloom filter can generate false positives (indicate that a query $q \in \mathbb{S}$ when it is absent). We will return to an analysis of false-positive rate after expanding on details of a bloom filter.

Given a search key x , if the search over \mathcal{B} is unsuccessful, it is guaranteed that $x \notin \mathbb{S}$. Otherwise, x may be present with a probability $1 - P$, where P is the false positive rate. Internally, a bloom filter \mathcal{B} is implemented as an array of M bits accompanied by h hash functions $\mathbf{H}_1, \mathbf{H}_2, \dots, \mathbf{H}_h$. To add an element $x \in \mathbb{S}$ to \mathcal{B} , each of the h hash functions map x to $[1, M]$, and thus the corresponding bits are set to 1. Concretely, $\mathcal{B}[\mathbf{H}_i(x)] = 1 \forall i \in [1, h]$.

To check the presence of an element x in \mathcal{B} , it suffices to check if $\exists i \in [1, h] \mathcal{B}[\mathbf{H}_i(x)] = 0$. If so, then it is guaranteed that $x \notin \mathbb{S}$ (otherwise, all the bits would be set to 1). Otherwise, the element *may be* present. Crucially, while creating the bloom filter incurs a one-time cost of $\mathcal{O}(|\mathbb{S}|h)$, the lookup can be done in $\mathcal{O}(h)$ time. Combined with the space requirements for \mathcal{B} , $M \ll |\mathbb{S}|$, a bloom filter provides an efficient way to determine if an element is absent from a set. The key elements in the design of a bloom filter are its size M , h hash functions $\mathbf{H}_1, \mathbf{H}_2, \dots, \mathbf{H}_h$, and the size of set \mathbb{S} over which search operations are to be performed.

Algorithm 2 Querying a bloom filter. The cost is a fixed constant $\mathcal{O}(h)$.

Given: \mathcal{B}, \mathbf{H}
for $i \leftarrow 1, 2, \dots, h$ **do** // $\mathcal{O}(h)$
 if $\mathcal{B}(\mathbf{H}_i(q)) = 0$ **then** // certainly absent
 return *False*
 end
end
/* Maybe present with a false positive rate p . */
return *True*

Algorithms 1 and 2 show the algorithms for creating and querying a bloom filter, respectively.

One of the biggest follies of a bloom filter are its false positive rates. Chang et al. (2004) proposed bucketed bloom filters to alleviate the false positive rate. In their method, each hash function \mathbf{H}_i maps to the indices $[(i-1) * m + 1, m]$, where $m = M/h$ is the number of bits in each bucket.

Let P be the rate of false positives, $|\mathbb{S}| = n$. Allowing each bucket of bloom filter to be 50% full, it can be shown that the number of elements $n \sim M^{\frac{(\ln 2)^2}{|\ln P|}}$ (Almeida et al., 2007). See Christensen et al. (2010) for a comprehensive analysis of false positive rate for classical implementation of bloom filters.

We next approximate the size of bloom filter required for storing all neighborhoods of a graph \mathcal{G} . Let $|\mathbb{V}|$ be the number of nodes in \mathcal{G} . Let d_{\max} be the max-degree of \mathcal{G} . Then, the number of neighborhoods \mathcal{N} of size p are upper-bounded by $|\mathbb{V}| * d_{\max}^{p-1}$. Clearly, this can be non-tractable for large, dense graphs. However, if d_{\max} is a fixed constant, then the number of neighborhoods is $\mathcal{O}(|\mathbb{V}|)$ (d_{\max}^{p-1} is absorbed in the constant). Thus, for such graphs, bloom filter can be tractably grown. Crucially, note that our goal is not to store all the graphs. Rather, we want to only approximately answer the membership queries in the graph.

B. Second-order sampling for generating the training data

For completeness, we now present the second order sampling method used by Grover & Leskovec (2016) that we adopt for generating the training data for our system.

Following the notation used by Grover & Leskovec (2016), let t be the previous node visited by the walk, and v be the current node (i.e., the walk just traversed $[t, v]$). The distribution over the next node x , $p(x | t, v)$, is given as $p(x | t, v) = \frac{\pi(x, t)}{\sum_{y \in \text{Adj}(v)} \pi(y, t)}$. Here, $\pi(x, t)$ is defined as follows:

$$\pi(x, t) = \begin{cases} \frac{1}{p} & \text{if } d_{tx} = 0 \\ 1 & \text{if } d_{tx} = 1 \\ \frac{1}{q} & \text{if } d_{tx} = 2 \end{cases}$$

The parameter p decides the likelihood of revisiting a node. Specifically, a low p will encourage the walk to go back to the node t recently visited. Similarly, q controls the likelihood of the walk visiting new nodes. A lower value of q will encourage the walk to move towards node that are farther away from the node recently visited, allowing higher exploration. Following Bojchevski et al. (2018), we set $p = q = 1$ to balance between the two properties. For

	FAST	SLOW	FLOWGEN
CORAML (500k)	76.8 (288)	92.2 (806)	90.8 (484)
CORAML (100M)	91.5 (50k)	96.7 (180k)	96.9 (110k)
CITeseer (500k)	90.9 (313)	94.6 (862)	93.3 (687)
CITeseer (100M)	96.1 (62k)	96.8 (172k)	96.5 (137k)
POLBLOGS (500k)	61.9 (309)	85.4 (854)	86.5 (686)
POLBLOGS (100M)	66.2 (48k)	93.8 (156k)	93.8 (108k)
PUBMED (500k)	58.36 (1200)	71.04 (854)	71.18 (686)
PUBMED (100M)	80.53 (253k)	92.09 (735k)	92.97 (509k)

Table 5. **Main results:** AUC for FAST, SLOW, and FLOWGEN, a combination of FAST-SLOW models. The time (seconds) taken by each setup is in parentheses. FLOWGEN closely matches or outperforms the larger model SLOW while taking a fraction of time.

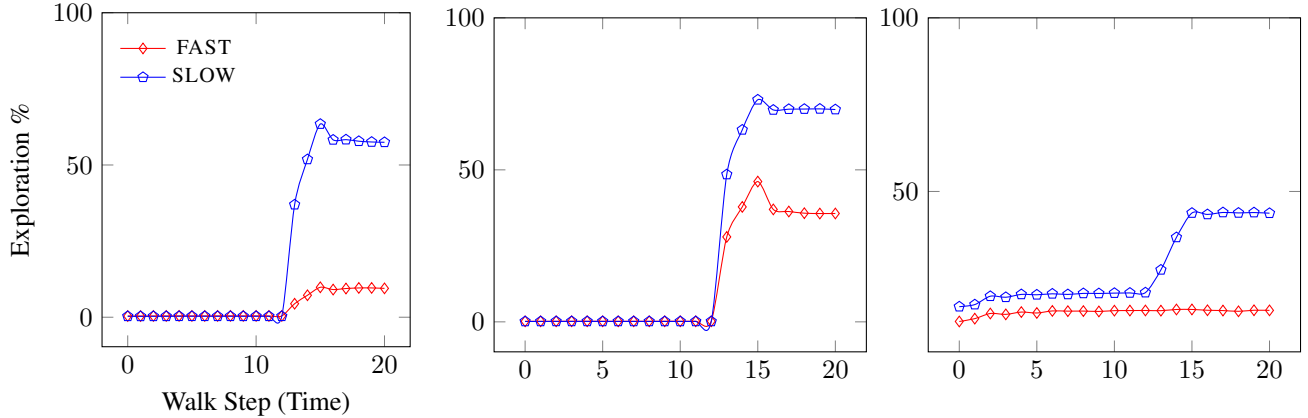


Figure 5. Exploration % (y-axis) vs. random walk step for CORAML (left), CITeseer (middle), and POLBLOGS (right). For all the graphs, the larger SLOW model explores once the walk exceeds a certain threshold, whereas the lighter FAST model repeats the training data.

more insights into the properties of second order random walk, please see Section 3.2 of (Grover & Leskovec, 2016).

C. Additional Results and Experimental Setup

Experimental Setup All the models were trained using a single Nvidia 2080-Ti GPU. During inference, we were able to fit both the models on a single GPU. We found that storing the models on separate GPUs erases some of the gains of FLOWGEN, due to required data transfer across machines. Implementation is done in PyTorch Lightning.³ Implementation of a number of evaluation and data generation scripts was derived from open-source implementation of Bojchevski et al. (2018).⁴

C.1. Graph structure metrics

Table 6 shows the structural metrics for all the graphs. For the mechanism to calculate these metrics, please see Ap-

pendix A of Bojchevski et al. (2018). Here, we instead provide an alternate and informal, high-level overview of each metric to help with interpretation of Table 6.

1. **Max. degree:** maximum degree across all nodes. Used to approximate the degree of density of the generated graph.
2. **Assortativity:** pearson correlation of degrees of connected nodes. Similar values for two different graphs indicates a similarity in topology.
3. **Triangle count:** number of triangles in a graph (set of three vertices connected to each other).
4. **Intra/Inter density:** fraction of edges that are part of the same community/fraction of edges that cross communities.
5. **Charac. path len** (characteristic path length): number of edges in the shortest path between any two vertices.
6. **Clustering coefficient:** For a given node v , let $\mathcal{N}(v)$ be its set of neighbors. Informally, clustering coefficient is the ratio of number of edges that exist within

³<https://www.pytorchlightning.ai/>

⁴<https://github.com/danielzuegner/netgan>

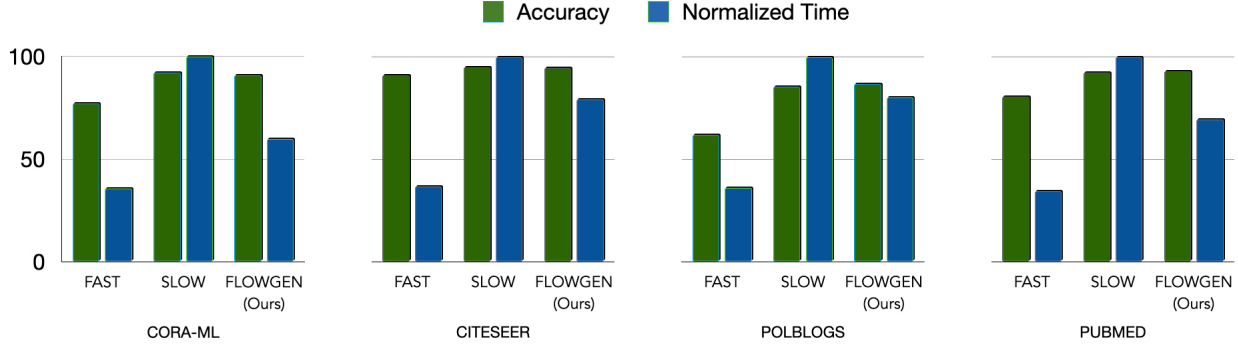


Figure 6. Average precision vs. time taken for the three graphs. The FAST and SLOW model speed-accuracy trade-off is apparent: FAST model is fast but less accurate (average precision $\sim 75\%$, compared to the SLOW model which is slower but has average precision of 92%). FLOW combines the strengths of the two modes: it achieves an accuracy of 90% while being $\sim 50\%$ faster than the SLOW model. Note that the time is normalized relative to SLOW (SLOW takes 100% of the time).

$\mathcal{N}(v)$, to the number of edges that can possibly exist within $\mathcal{N}(v)$.

detected early on for all the cases (within 4 steps), and then fluctuates around a mean value.

C.2. Performance of FLOWGEN with scale

How does the performance of FLOWGEN change as the scale of data increases? To test this, we vary the number of random walks n generated during inference to recreate the graph. The results are shown in Figure 7. FLOWGEN matches or outperforms SLOW, while being consistently faster across the number of walks. Table 8 shows the AUC for different graphs for 500k and 100M walks.

C.3. Using entropy for deciding the switch

Our method of switching from FAST to SLOW model relies on the presence of the walk in training set. This can be seen We also experiment with using entropy for deciding the switch, but found it ineffective in determining exploration vs. exploitation Appendix (C.3). Recall that we are using an auto-regressive language model for generating the walks. Thus, at each step i , the model generates a distribution over the next node, $p(v_i | v_1, v_2, \dots, v_{i-1})$. Thus, for a well calibrated model, in the exploitation phase, when the model is still generating walks from the training set, the entropy of this distribution will be fairly low (the model will be confident about the next node), and that the entropy will increase further in the walk. If that was the case, the entropy of the distribution can be a useful indicator of the switching point. We investigate the same in this section.

Specifically, we generate a walk of length 32, and for each step i , we calculate the entropy of the distribution $p(v_i | v_1, v_2, \dots, v_{i-1})$. The average entropy at each step is calculated, and the knee (Satopaa et al., 2011) of the entropy plot is used as the switching point. The results are shown in Figures 8 and 9. As the Figures show, the knee point is

Graph	Type	Max. degree	Assort-activity	Triangle Count	Power law exp.	Inter-comm. unity density	Intra-comm. unity density	Cluster- ing coeff.	Charac. path len.
CORAML	FAST	216.0	-0.08186	2461	1.84745	0.00129	0.00058	0.00317	5.59302
CORAML	SLOW	200.0	-0.07949	2143	1.84531	0.0013	0.00055	0.00333	5.40631
CORAML	FLOWGEN	200.0	-0.080	2,351	1.84	0.00129	0.00056	0.00395	5.50565
CITSEER	FAST	59.0	-0.04444	427	2.19731	0.00114	0.00025	0.01601	9.73914
CITSEER	SLOW	55.0	-0.04329	437	2.18366	0.00114	0.00026	0.0195	9.80901
CITSEER	FLOWGEN	61.0	-0.03117	455	2.17116	0.00116	0.00025	0.01872	9.87617
POLBLOGS	FAST	254.0	-0.30609	44428	1.43388	0.00534	0.01406	0.00438	2.85113
POLBLOGS	SLOW	273.0	-0.23833	52742	1.43739	0.0054	0.014	0.0047	2.80242
POLBLOGS	FLOWGEN	289.0	-0.25944	49204	1.43222	0.00541	0.01397	0.00442	2.79202
PUBMED	FAST	115.0	-0.1228	4970	2.29702	4e-05	0.00015	0.00348	6.84598
PUBMED	SLOW	106.0	-0.14983	4089	2.2487	4e-05	0.00015	0.00321	6.76372
PUBMED	FLOWGEN	111.0	-0.14689	4172	2.25055	4e-05	0.00015	0.00324	6.76702

Table 6. Structural metrics for all graphs used in this work. FLOWGEN closely matches SLOW, but takes only a fraction of time.

Method	CORAML		CITSEER		PUBMED		POLBLOGS	
	AUC	AP	AUC	AP	AUC	AP	AUC	AP
Adamic/Adar	92.16	85.43	88.69	77.82	84.98	70.14	85.43	92.16
DC-SBM	96.03	95.15	94.77	93.13	96.76	95.64	95.46	94.93
node2vec	92.19	91.76	95.29	94.58	96.49	95.97	85.10	83.54
VGAE	95.79	96.30	95.11	96.31	94.50	96.00	93.73	94.12
NetGAN (500K)	94.00	92.32	95.18	91.93	87.39	76.55	95.06	94.61
NetGAN (100M)	95.19	95.24	96.30	96.89	93.41	94.59	95.51	94.83
FLOWGEN (100M)	96.93	97.22	96.8	97.45	93.0	91.16	93.8	95.05

Table 7. Comparison of FLOWGEN with baselines on link prediction task for six different graphs.

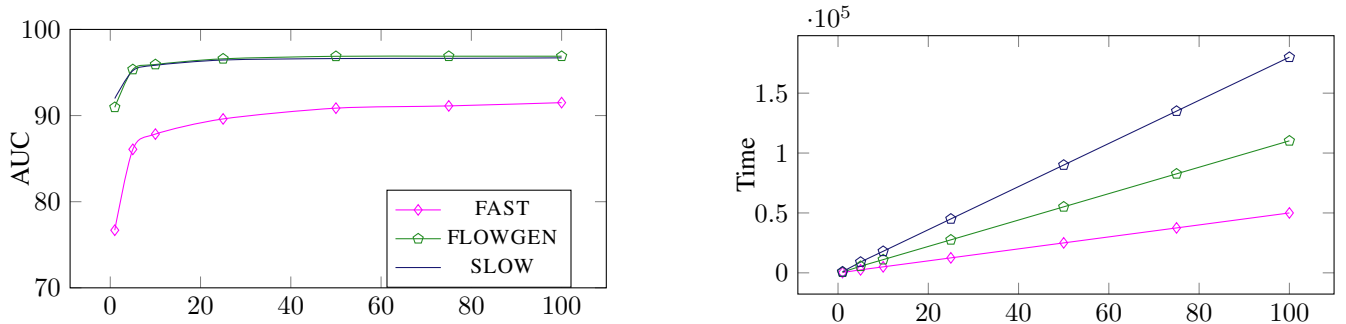


Figure 7. AUC and time taken (y-axis) for the three models for CORAML, as the number of random walks sampled increases from 500k to 100M.

	FAST		SLOW		FLOWGEN	
	AUC	Time (s)	AUC	Time (s)	AUC	Time (s)
CORAML (500k)	76.8	288	92.2	806	90.8	484
CORAML (100M)	91.5	50k	96.7	180k	96.9	110k
CITSEER (500k)	90.1	313	94.6	862	93.3	687
CITSEER (100M)	96.1	62k	96.8	172k	96.5	137k
POLBLOGS (500k)	61.9	309	85.4	854	86.5	686
POLBLOGS (100M)	66.2	48k	93.8	156k	93.8	108k
PUBMED (500k)	61.9	309	85.4	854	86.5	686
PUBMED (100M)	80.5	253k	92.1	735k	93.0	509k

Table 8. Performance of SLOW, FAST, and FLOWGEN for different number of sampled random walks: FLOWGEN is competitive across scale.

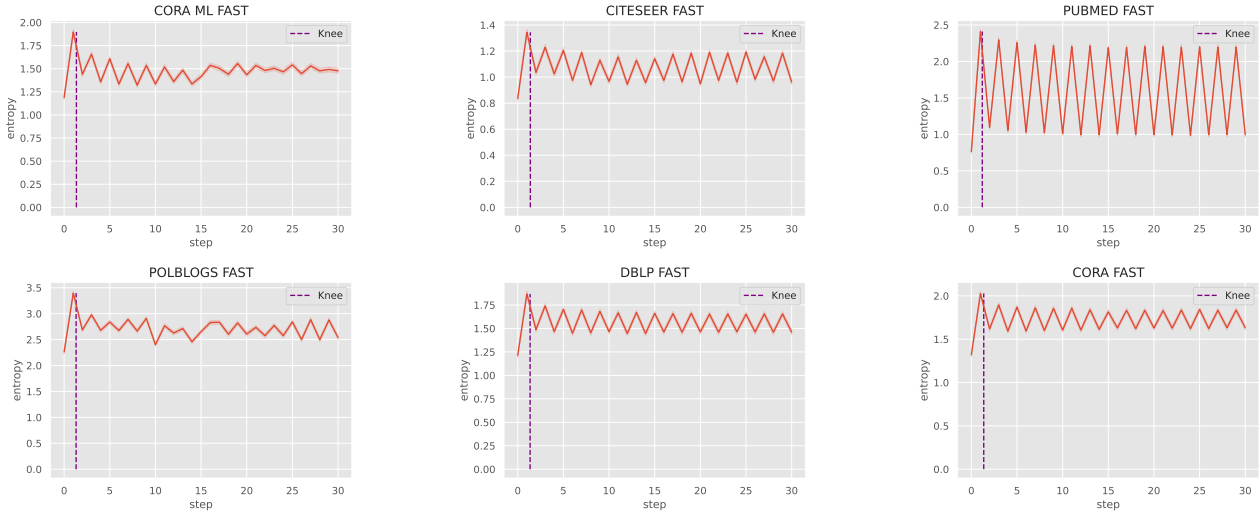


Figure 8. Entropy analysis for the FAST models

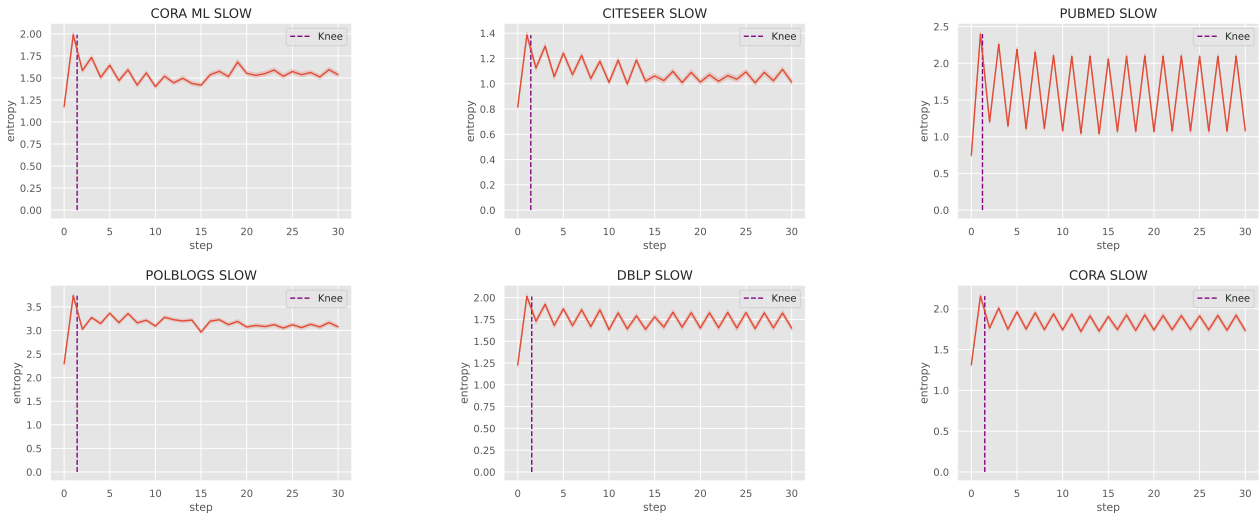


Figure 9. Entropy analysis for the SLOW models